



10IKC-230

AN UPDATED GEOLOGICAL MODEL OF THE MISERY KIMBERLITE COMPLEX, EKATI MINE, NORTHWEST TERRITORIES, CANADA

Webb* KJ¹, Hetman CM^{1,3}, Nowicki TE¹, Harrison S², Carlson J², Parson S^{2,3} and Paul JL¹

¹Mineral Services Canada, North Vancouver, Canada; ²BHP Billiton, Yellowknife, Canada; ³now with Northern Superior Resources, Sudbury, Canada

INTRODUCTION

The Misery kimberlite complex forms part of the Lac de Gras kimberlite province on the Slave Craton in the Northwest Territories of Canada (Fig. 1; Nowicki et al., 2004). It was emplaced at approximately 56 Ma at the contact between biotite schist and granite when the area was overlain by poorly consolidated mudstones and shale. Misery was mined from 2001 to 2005 by open cut methods, and a pushback expansion was approved in mid-2011. Waste stripping is underway with first ore production expected in 2015. The occurrence is one of the highest grade primary diamond deposits in the world with an average grade of approximately 4 ct/T.

The original geological model of the complex comprised nine bodies, including steep sided pipes infilled with volcanoclastic kimberlite as well as dykes and irregular intrusions of coherent kimberlite (Fig. 2; Mustafa et al., 2003). The model was constructed using mining, drill core geology, bulk sampling and indicator mineral composition data. However, while a significant amount of drilling and sampling data were available for the upper portion of the main ore body, the Misery Main Pipe, limited data were available for most of the peripheral bodies and at depth, and hence these were not reliably constrained.

With the expansion of the Misery open pit, it has become important to better determine the morphology, internal geology and grade potential of some of these peripheral bodies, in particular the Southwest Extension (SWE) and South Pipe. Given the location of these bodies with respect to the open pit design, and their weaker rock strength relative to the host rock, they pose a geotechnical risk during mining. These sources also have potential to become feed to the process plant as diamond prices increase, presenting upside to the Misery expansion project.

Thus, between 2007 and 2010 additional delineation and bulk sample drilling was undertaken on the Main Pipe, SWE and South Pipe, and these data form the basis of a revised geological model for the three bodies (Fig. 3). It is now apparent that the two peripheral bodies are larger than originally modelled and the relationship with the Main Pipe is complex. Representative indicator mineral and micro-diamond samples were taken from these drill holes to help constrain the internal geology and to assess the relative diamond grade potential of the bodies.

This contribution presents a summary of the key results of this work, including an updated geological model, comment on internal variation in petrographic, indicator mineral and microdiamond characteristics, and the significance of these with respect to possible diamond grade variation.

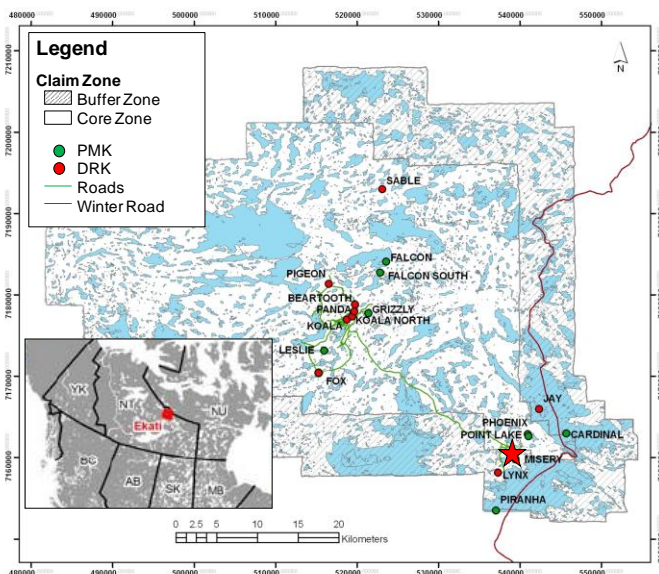


Figure 1: Map showing the location of the Misery complex in relation to other kimberlites on the EKATI claims block. Inset: map of north-western Canada showing the location of the EKATI property. PMK = potential mineralization kimberlites; DRK = declared resource kimberlites.

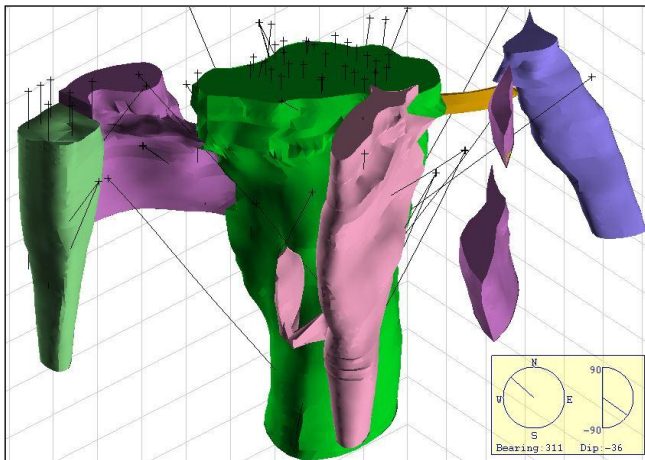


Figure 2: Three-dimensional image of the 2003 geological model of the Misery kimberlite complex (Mustafa et al., 2003), showing the traces of core drill holes on which the model was based.

GEOLOGY AND EVOLUTION OF MODEL

The revised geological model for the Main Pipe, SWE and South Pipe based on data available in 2010 is illustrated in Figure 3. A summary of the main differences between the 2003 and 2010 models is shown in Table 1. No significant additional work was undertaken on other bodies in the Misery kimberlite complex and these are not discussed further in this contribution.

The steep sided ~1.5 ha Misery Main Pipe is the largest body in the complex. Historically modelled as a single geological domain, the pipe infill has now been divided into three separate sub-domains, occupying the northern, southern and deep (below ~440 m) portions of the pipe: KIMB3-north, KIMB3-south and KIMB4, respectively. KIMB3 is a fine to medium grained, variably bedded, dominantly olivine-rich (25-70%) volcanoclastic kimberlite (VK) interpreted to have formed by resedimentation of pyroclastic kimberlite (hence, RVK). Melt-free olivine crystals, crustal xenoliths (including distinct deformed mud clasts), accretionary clasts, VK autoliths, mantle xenocrysts and rare subround melt-bearing pyroclasts occur in a mud-rich interclast matrix. Macroscopically KIMB3 closely resembles the main RVK in the adjacent SWE (see further comment below). KIMB3 is divided into two sub-domains based primarily on grade: KIMB3-north yields roughly double the grade of KIMB3-south, with average sample grades trending from 5 to 2 c/t north to south. This partly reflects different mud contents, but may also result from resedimentation of different PK deposits (see below). KIMB 4 occurs in the lowermost portion of the modelled Main Pipe; this variably bedded RVK is notably finer-grained than KIMB3 with lower olivine and basement xenolith contents.

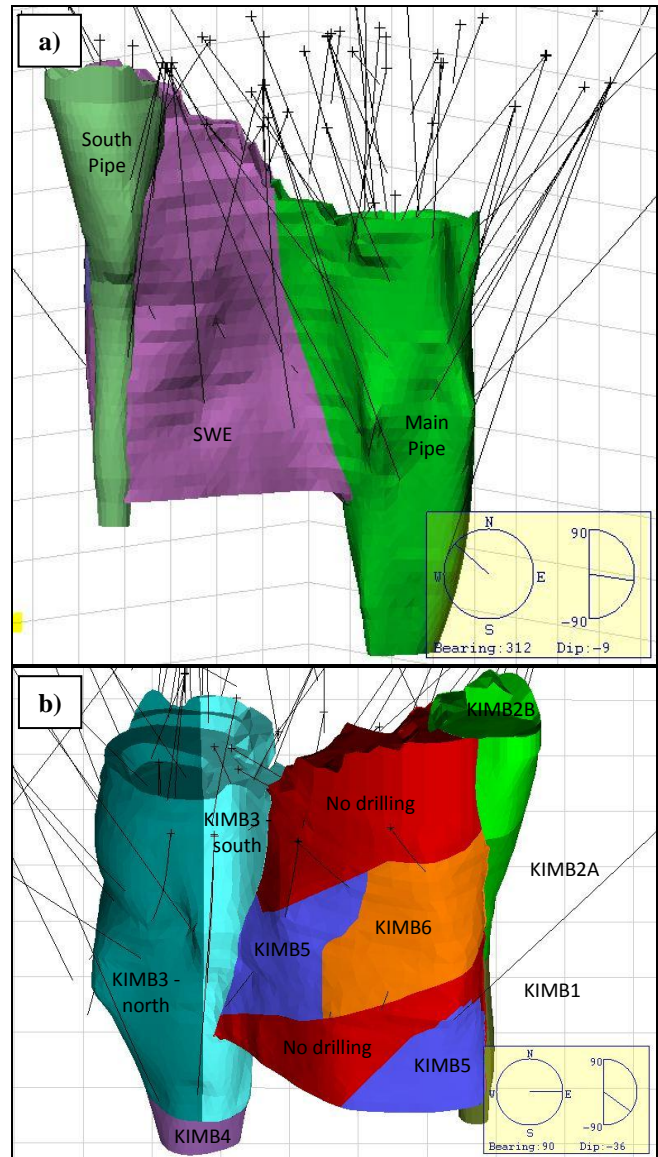


Figure 3: Three-dimensional image of the 2010 geological model of the Misery Main Pipe, SWE and South Pipe, showing the traces of core drill holes on which the model is based. a) View as in Fig. 2 showing revised model for the Main Pipe, SWE and South Pipe; b) View of revised model from the west showing internal domains defined based on rock type.

Originally modelled as an elongated shallow ‘bridge’ of coherent kimberlite (CK) between the Main Pipe and South Pipe (Fig. 2), the SWE has now been defined as a narrow steep sided body that extends to at least 380 m depth and is infilled with at least two broad varieties of RVK. The volume of the revised body is more than five times that of the previous model. KIMB5, the dominant infill, occurs adjacent to and appears similar to KIMB3 in the Main Pipe. KIMB6 overlies and occurs between KIMB5 and the South Pipe; this well-bedded mud-rich RVK contains common pale sediment xenoliths. The internal geology in undrilled parts of the SWE is currently undifferentiated (Fig. 3).

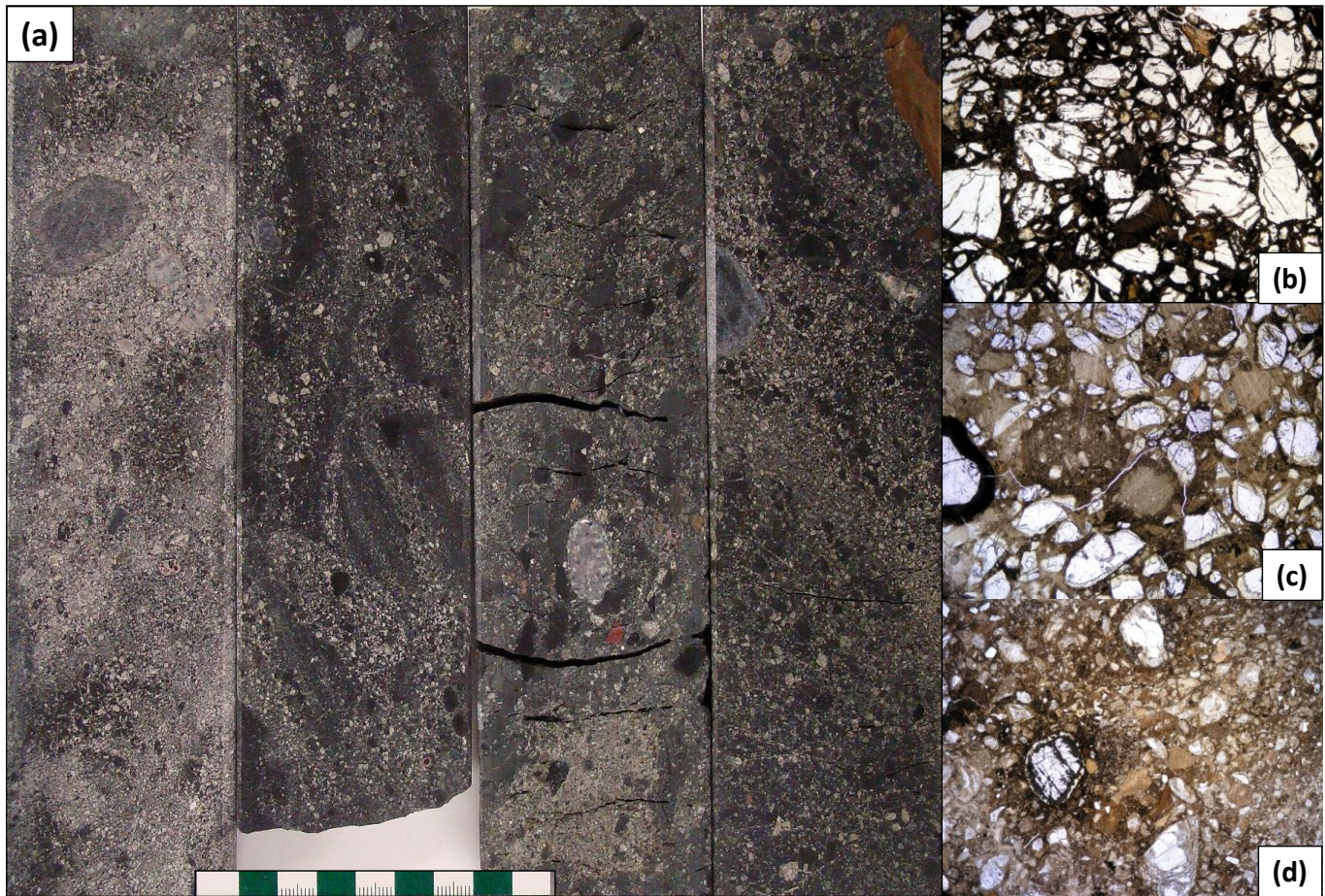


Figure 4: (a) Polished drill core slabs of KIMB3 showing the characteristic textural heterogeneity; MGT51; 314.6 m, 318.95 m, 330.15 m, 342.75 m (left to right), scale in centimeters; photomicrographs of (b) olivine-rich KIMB3 (314.6 m); (c) an accretionary clast (left centre) in KIMB3 (342.75 m); note also the paucity of melt-bearing pyroclasts; (d) a fine grained poorly sorted mud-rich bed in KIMB6 (MGT53, 296 m). All fields of view = 7 mm.

Table 1: Summary of key differences between the 2003 and 2010 geological models for the Misery Main Pipe, SWE and South Pipe. Domains in the 2010 model comprise RVK, with the exception of KIMB1, which includes interbedded pyroclastic kimberlite.

Body	2003		2010 (remaining)		Total
	Domain	Volume (Mm ³)	Domain	Volume (Mm ³)	
Main	Main (RVK)	4.09	KIMB3-n	1.86	3.15
			KIMB3-s	1.21	
			KIMB4	0.08	
SWE	SWE (CK)	0.55	KIMB5	0.78	2.94
			KIMB6	0.52	
			Unknown	1.64	
South	South (RVK)	0.54	KIMB1	0.10	0.77
			KIMB2A	0.23	
			KIMB2B	0.44	

The steep sided ~0.4 ha South Pipe is infilled to 260 m depth with variably mud- and olivine-rich RVK. In the updated model this material has been subdivided into lower and upper domains, known as KIMB2A and KIMB2B respectively, based on the relative abundance of matrix mud and sedimentary xenoliths. The lowermost portion of the South Pipe (defined as the KIMB1 domain) is occupied by medium to coarse grained, generally massive resedimented volcanoclastic kimberlite with lesser interbedded pyroclastic kimberlite.

MODEL CONFIRMATION WITH INDICATOR MINERALS AND MICRODIAMONDS

Contrasting volcanoclastic kimberlite types can generally be distinguished based on differences in the character of melt-bearing pyroclasts and other juvenile and xenolithic components. At Misery, the components of the main RVKs infilling the Main Pipe and SWE are the same or extremely similar and melt-bearing pyroclasts occur in very low



proportions. In particular, KIMB3 and KIMB5 have a very similar overall petrographic appearance. Thus, in order to increase confidence in the geological model and to assess whether any significant differences exist between KIMB3, KIMB5 and KIMB6, indicator mineral and microdiamond analysis was undertaken on representative samples of these main kimberlite types (or domains) defined for the Misery Main Pipe and SWE bodies.

Indicator mineral compositions

Ten samples were analysed by the standardised Mantle MapperTM method to obtain representative quantitative indicator mineral abundance and composition data. The results indicate substantial internal variability in indicator mineral characteristics within the different kimberlite domains defined to date, suggesting potential for significant local variation in diamond content. However, some consistent and significant differences in key indicator mineral features are evident, suggesting overall differences in the nature of the contained mantle-derived component and the diamond potential of each domain. These are reflected primarily in variations in the proportion of diamond-associated peridotitic (G10D) and eclogitic/websteritic (G3D/G4D) garnet present (Figs. 5 and 6). Based on indicator mineral results, the relative interest rating, from highest to lowest, of the main kimberlite types is: KIMB3-north > KIMB3-south > KIMB5 ≥ KIMB6.

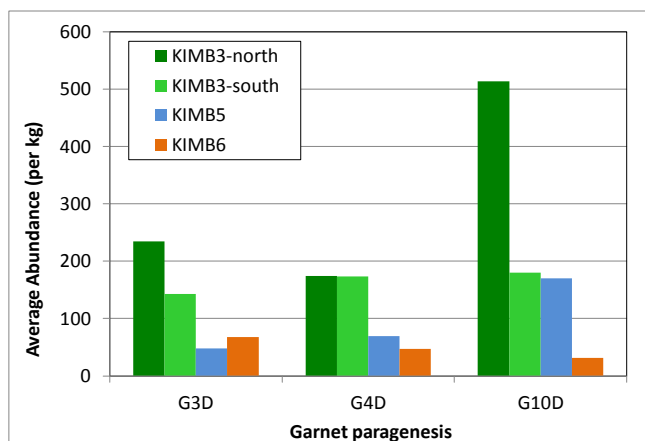


Figure 5: Bar chart illustrating variations in the abundance of different diamond-associated garnet types in the Misery domains sampled for indicator mineral analysis. The graphs represent average abundances for all samples from a given domain. Garnet parageneses based on Grütter et al. (2006).

Microdiamond results

Microdiamond data are available for 10 samples of kimberlite types in the Main Pipe and SWE, in most cases corresponding broadly with intervals sampled for indicator mineral analysis. Individual samples range in size from

approximately 50 to 250 kg and were processed by caustic fusion, followed by sieving and weighing of diamonds extracted from the residue. The results indicate significant differences in stone frequency (stones per tonne) and micro-diamond grade (“micro-grade”; carats per tonne) between samples of the same kimberlite types but, as in the case of indicator mineral data, also demonstrate significant overall differences between kimberlite types. A single sample of KIMB3-north yielded the highest stone frequency and micro-grade of all samples, consistent with its known high macrodiamond grade. Three samples of KIMB3-south yielded significantly lower stone frequencies and variable but consistently lower micro-grades than KIMB3-north. Samples of KIMB5 (4) and KIMB6 (2) display similar ranges in stone frequency to KIMB3-south but the micro-grade of the KIMB5 samples is substantially lower than that of KIMB3-south, and KIMB6 samples have considerably lower micro-grades than KIMB5. These variations reflect what appear to be consistent significant differences in diamond size frequency distribution, with KIMB3 being the coarsest, KIMB5 intermediate and KIMB6 displaying a distinctly finer size distribution (Fig. 7). The microdiamond results support the distinction between the main rock types identified in the Main Pipe and SWE. They suggest that the grade difference between KIMB3-south and KIMB3-north stems primarily from a lower overall concentration of diamonds, whereas in the case of KIMB5 and KIMB6 this is compounded by finer grained diamond populations.

SUMMARY AND CONCLUSIONS

Detailed work has led to a major revision in the interpreted geology of portions of the Misery kimberlite complex. In particular, the SWE has been expanded considerably and shown to comprise at least two types of RVK.

Due to the similarity in texture, components and dominant pyroclastic and resedimentation processes by which they formed, it is very difficult to distinguish the main RVK types infilling the Main Pipe (KIMB3) and SWE (KIMB5), despite the fact that available grade data indicate significant differences in diamond content.

Indicator mineral and microdiamond data provide support for grade differences and help map the distribution of the main kimberlite types present. These data provide valuable information on the relative diamond potential of each of the modelled domains, providing an important basis for further evaluation of the SWE.

This study highlights the importance of an integrated geological and mineralogical approach for distinguishing kimberlite types and also illustrates the evolution of geological models with the addition of new, multi-disciplinary datasets.

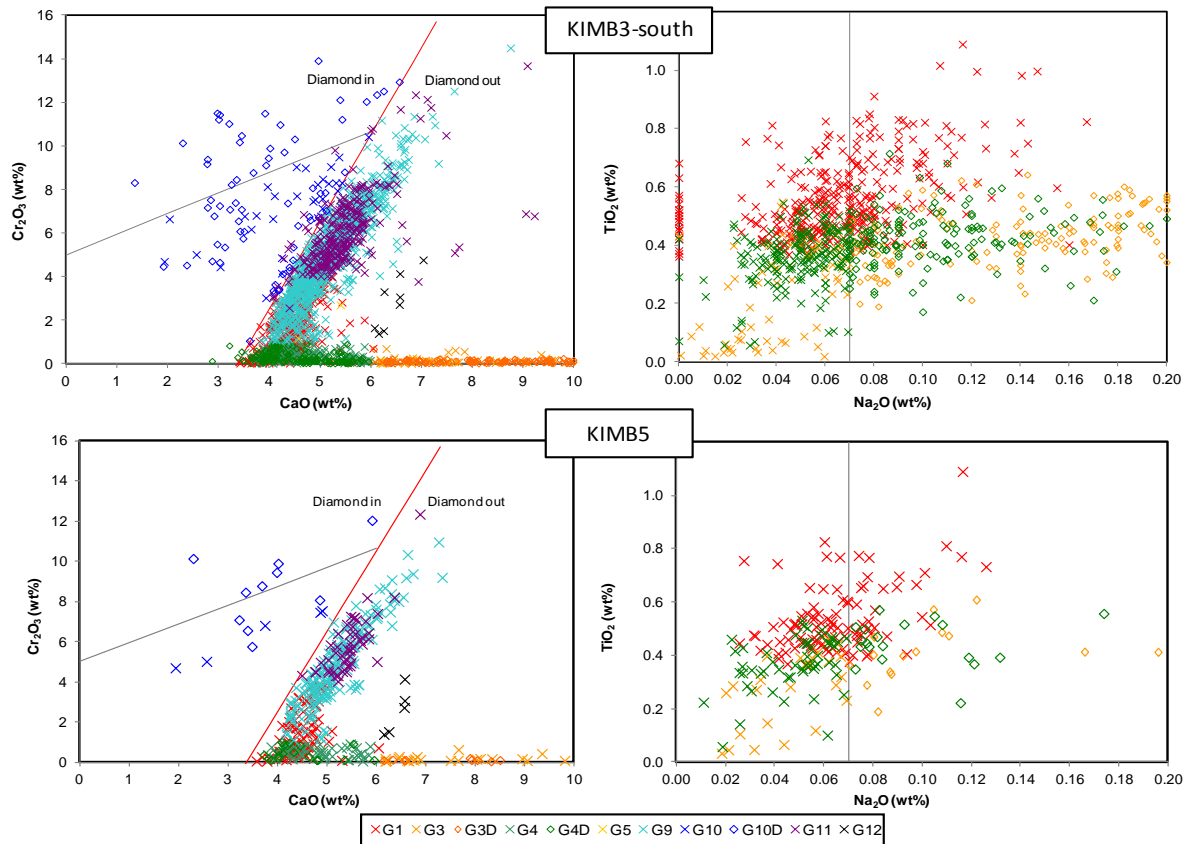


Figure 6: Standard garnet $\text{Cr}_2\text{O}_3 - \text{CaO}$ and $\text{TiO}_2 - \text{Na}_2\text{O}$ plots showing the compositional range of garnets from the KIMB3-south and KIMB5 domains. Garnets are colour coded by paragenesis on the basis of the Grütter et al. (2006) classification. Samples from KIMB5 are characterised by lower proportions of diamond associated peridotitic (G10D) and eclogitic (G3D/G4D) garnet than KIMB3-south. Reference lines: “Diamond in / diamond out” line of Gurney (1984) – red; “graphite diamond constraint” of Grütter et al. (2006) – grey line on $\text{Cr}_2\text{O}_3 - \text{CaO}$ plots; 0.07 wt% Na_2O lower cut-off for diamond inclusion type eclogitic garnet (McCandless and Gurney, 1989) - grey line on $\text{TiO}_2 - \text{Na}_2\text{O}$ plot.

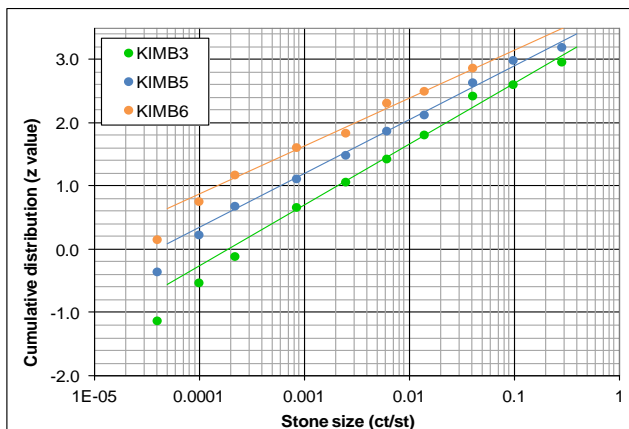


Figure 7: Cumulative size distribution plot showing combined microdiamond datasets for the KIMB3, KIMB5 and KIM6 domains. The graph shows the proportion of diamonds (represented by normal scores on the y axis), below a given stone size (in carats per stone, plotted on a log scale on the x axis). Normal scores of 0, 1 and 2 represent 50%, 84% and 98% of the data, respectively. Lines represent graphically fitted log-normal models for each population. The graph indicates that 6% ($Z=1.6$) of the stones in the KIMB3 diamond population exceed ~ 0.01 carats per stone, whereas only 2% ($Z=2$) and 1% ($Z=2.4$) of the stones in the KIMB5 and KIMB6 populations exceed this value, respectively.

REFERENCES

- Grütter, H.S., Latti, D. and Menzies, A.H. (2006). Cr-saturation arrays in concentrate garnet compositions from kimberlite and their use in mantle barometry. *Journ. Petrol.*, 47, 801-820.
- Gurney, J.J. (1984). A correlation between garnets and diamonds in kimberlites. In: Glover, J.E. and Harris, P.G. (Eds.), *Kimberlite Occurrence and Origin: A basis for conceptual models in exploration*, Geology Dept and University Extension, Univ. of W. Australia, Publ. 8., 143-166, Blackwell Scientific Publications, Perth.
- McCandless, T.E. and Gurney, J.J. (1989). Sodium in garnet and potassium in clinopyroxene: criteria for classifying mantle xenoliths. In: Ross, J. (Ed.), *Kimberlites and Related Rocks*, Vol. 2, Geol. Soc. Austr., Spec. Publ. 14, 827-832, Blackwell Scientific Publications, Perth.
- Mustafa, J., Nowicki, T., Oshust, P., Dyck, D., Crawford, B. and Harrison, S., 2003. The geology of the Misery kimberlite, EKATI Diamond Mine™, Canada. Long Abstracts, 8th International Kimberlite Conference, Victoria, Canada.
- Nowicki, T., Crawford, B., Dyck, D., Carlson, J., McElroy, R., Oshust, P., Helmstaedt, H., 2004. The geology of kimberlite pipes of the EKATI property, Northwest Territories, Canada. *Lithos*, 76 (1-4): 1-27.